J Fluoresc (2015) 25:127–136
DOI 10.1007/s10895-014-1489-6

ORIGINAL PAPER

A Combined Experiment and Computation Study of the Fused Polycyclic Benzimidazole Derivatives

Mininath S. Deshmukh · Archana A. Bhagwat · Nagaiyan Sekar

Received: 29 September 2014 / Accepted: 2 December 2014 / Published online: 10 December 2014

Abstract Novel fused polycyclic benzimidazole derivatives were synthesized from dimethyl 4,5-diaminophthalate/dimethyl 3,4-diaminophthalate with aromatic anhydride **(a-b)** by condensation. The UV-Visible absorption and fluorescence emission spectra of the dyes were studied in solvents of differing polarity. The dyes were characterized by the spectral analysis. Density Functional Theory computations have been used to derive more understanding of structural, molecular, electronic and photophysical parameters of the push-pull dyes. The computed absorption wavelength values were observed to be in good agreement with the experimental results. The second order hyperpolarizability (β_o) values were computed by Density Functional Theory and found to be in the range of 67.16×10^{-31} to 107.76×10^{-31} e.s.u.

Keywords Polycyclic benzimidazole · Solvatochromism · Photo-physics · Hyperpolarizability · DFT · TD-DFT

Introduction

The importance of the imidazo[2,1-a]isoindolone skeleton is well recognized as a subunit due to its significance as a wide range of synthetic pharmaceutical compounds. Some of these compounds are patented and have been reported to have a wide range of biological activities like analgesic, antifungal, anti-inflammatory, antipyretic, hypertensive, and psychostimulant, [1, 2] blood pressure lowering, spasmolytic, anti tussive and tranquilizer properties, [3] and used in the treatment of rheumatism. [4]. Also, they are useful intermediates in synthetic organic chemistry, particularly in the amplification of imidazo[2,1-a]isoindolol-based anorectics, [2, 5, 6]central nervous system (CNS) stimulants [7, 8] and antidepressants, [9] respectively. This class of compounds has also confirmed to be highly effective plant growth regulating agents [10] with effects on the plant budding process [11–13]. Most recently reported benzimidazo[2,1-a]isoindolonesunit have been comparable shown their biological activities evaluation with Batracylin anti-tumor activities [14] as well as their ability to bring unscheduled DNA synthesis in rathepatocytes [15, 16].

Along with biological importance, the benzo[4,5]imidazo[2,1-a]isoindolone unit are effective candidates in both as organic pigments [17, 18] and n-type organic semiconductors [19, 20]. Because of their stability, high light absorptivity and good electron transportation process of these derivatives have been extensively studied for developing different derivatives in organic electronics. The benzo[4,5]imidazo[2,1-a]isoindolone derivatives have already shown to be the promising candidates in optoelectronic device [21], light-emitting diodes [22, 23], organic thin-film transistors (OTFTs) [24, 25], organic photovoltaic's (OPVs) [26, 27], organic electronics [28] and Organic Field Effect Transistors (OFET) [29–31].

To design and synthesis of such compounds having considerable molecular properties, such as reduction/oxidation potentials, band gap between HOMO-LUMO, and solid-state crystal packing to achieve materials with enhanced transport properties is an important area of research [27]. In recent years, computational approach using Density Functional Theory (DFT) and Time Dependent Density Functional

Electronic supplementary material The online version of this article (doi:10.1007/s10895-014-1489-6) contains supplementary material, which is available to authorized users.

M. S. Deshmukh · A. A. Bhagwat · N. Sekar (✉)
Tinctorial Chemistry Group, Institute of Chemical Technology (Formerly UDCT), N. P. Marg, Matunga, Mumbai 400 019, Maharashtra, India
e-mail: n.sekar@ictmumbai.edu.in

N. Sekar
e-mail: nethi.sekar@gmail.com

Theory (TD-DFT) has been effective tool to understand the molecular basis of photophysical as well as other electronic properties driven by the interaction of electromagnetic impulses with organic compounds [32].

In this paper, traditional synthesis of benzo[4,5]imidazo[2,1-a]isoindolone derivatives involving the reaction between dimethyl 4,5-diaminophthalate **(1)** or dimethyl 3,4-diaminophthalate **(2)** and an aromatic anhydrides **(a-b)** and their photophysical properties are reported. Density functional theory computations [B3LYP/6-31+G(d)] were used to study the geometrical and electronic properties of the synthesized molecules and compared with the experimentally obtained photophysical data.

Experimental Section

Materials and Methods

All the commercial reagents and the solvents were purchased from S. D. Fine Chemicals Pvt. Ltd. and were used without purification. The reaction was monitored by TLC using on 0.25 mm silica gel 60 F_{254}precoated plates, which were visualized with UV light. Melting points were measured on standard melting point apparatus from Sunder industrial product Mumbai and are uncorrected. FT-IR spectra were recorded on Jasco 4100 using ATR accessory. ^{1}H-NMR spectra were recorded on VARIAN Inc. (USA) 500-MHz instrument using TMS as an internal standard and $CDCl_3$/DMSO-d_6 as the solvent at room temperature. Mass spectra were recorded on Finnigan mass spectrometer. Simultaneous DSC-TGA measurements were performed out on SDT Q 600 v8.2 Build 100 model of TA instruments Waters (India) Pvt. Ltd. The UV-visible absorption and emission spectra were performed on a Perkins-Elmer Lamda 25 and Varian Cary Eclipse at room temperature respectively. Quantum yields were obtained by using quinine sulfate (0.54 in 1 M H_2SO_4) as reference [33].

Computational Methods

The ground state (So) geometries of the synthesized compounds were optimized in vacuum using Density Functional Theory (DFT) [34]. The functional used was B3LYP. The B3LYP method combines Becke's three parameter exchange functional (B3) [35] with the nonlocal correlation functional by Lee, Yang, and Parr (LYP) [36]. The basis set used for all the atoms was 6-31+G(d), the latter has been justified in the literature [37–39] for the current investigation. The vibrational frequencies at the optimized structures were computed using the same method to verify that the optimized structures correspond to local minima on the energy surface [40]. The vertical excitation energy and oscillator strengths at ground state equilibrium geometries were calculated by using TD-DFT at the same hybrid functional and basis set [41–43]. The low-lying first singlet excited states (S1) of dyes was relaxed using TD-DFT to obtain its minimum energy geometry. The difference between the energies of the optimized geometries at the first singlet excited state and the ground state was used in computing the emissions [44, 45]. Frequency computations were also carried out on the optimized geometry of the low-lying vibronically relaxed first excited state of the conformers. All the computations in solvents of different polarities were carried out using the Polarizable Continuum Model (PCM) [46]. All electronic structure computations were carried out using the Gaussian 09 program [47].

Synthesis and Characterization

The synthetic scheme for the preparation of benzo[4,5]imidazo[2,1-a]isoindolone **(3a–3b** and **4a–4b)** derivatives are shown in Scheme 1. Dimethyl 4,5-diaminophthalate **(1)** and dimethyl 4,3-diaminophthalate (**2**) were prepared by the reported procedure [48] from 4-nitrophthalic acid.

General Procedure for the Preparation of Isoindolone

Diamino-dimethyl phthalate **(1** or **2)** 0.5 g (2.2 mmol) and different aromatic anhydride **(a–b)** (2.2 mmol) were dissolved in acetic acid (5 mL), and the reaction mixture was refluxed for 6 h. The mixture was poured on the crushed ice and the precipitate obtained was filtered, washed with cold water till neutral pH and dried to afford **3a–3b** and **4a–4b**. The product was recrystalized from ethanol.

*Dimethyl 11-oxo-11H-benzo[4,5]imidazo[2,1-a]isoindole-7,8-dicarboxylate (***3a***)* Yield: 75 %; Melting point: 136–138 °C; Mass m/z: 337.44 $[M+H]^+$; ^{1}H NMR (DMSO-d_6, 300 MHz): δ 8.20 (d, 1H, Ar-H, J=7.8 Hz), 8.08 (s, 2H, Ar-H), 7.53 (t, 1H, Ar-H, J=7.2 Hz),7.20 (d, 1H, Ar-H, J= 7.2 Hz),7.11 (t, 1H, Ar-H, J=7.8 Hz),3.87 (s, 6H, -

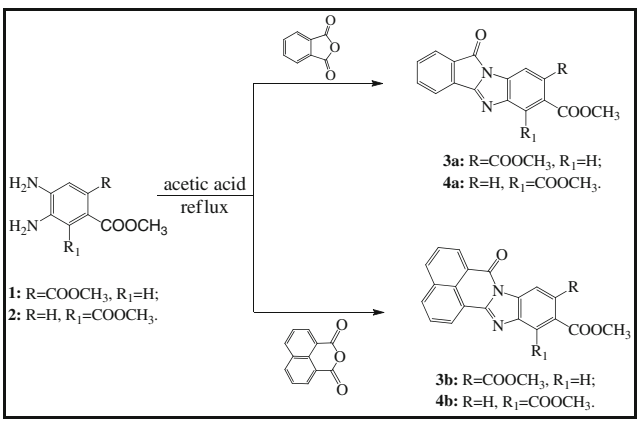

Scheme 1 Synthesis of benzo[4,5]imidazo[2,1-a]isoindolonederivatives

OCH_3);FTIR: 1716 (C=O stretching), 1657, 1630 (C=C, C=N stretching), 1592, 1436 (C-C aromatic stretching), 1337, 1310, 1234 (C-N, C-O stretching) cm^{-1}.

*Dimethyl 7-oxo-7H-benzo[de]benzo[4,5]imidazo[2,1-a]isoquinoline-10,11-dicarboxylate (***3b***)* Yield: 80 %; Melting point: 162–164 °C; Mass m/z: 387.20 $[M+H]^+$; ^1H NMR (DMSO-d_6, 300 MHz): δ 8.81 (m, 2H, Ar-H), 8.64 (d, 1H, Ar-H, *J*=8.1 Hz),8.49 (d, 1H, Ar-H, *J*=8.4 Hz),8.18 (s, 2H, Ar-H),8.21 (dd, 2H, Ar-H, *J*=7.8 Hz and *J*=8.7 Hz),3.93 (s, 3H, -OCH_3), 3.90 (s, 3H, -OCH_3);FTIR: 1735, 1710 (C=O stretching), 1621, 1593(C=C, C=N stretching), 1542, 1428(C-Caromatic stretching), 1344, 1325, 1260(C-N, C-Ostretching) cm^{-1}.

*Dimethyl 11-oxo-11H-benzo[4,5]imidazo[2,1-a]isoindole-6,7-dicarboxylate (***4a***)* Yield: 72 %; Melting point: 128–130 °C; Mass m/z: 337.28 $[M+H]^+$; FTIR: 1739, 1718 (C=O stretching), 1615, 1574 (C=C, C=N stretching), 1502, 1429 (C-Caromatic stretching), 1371, 1318, 1276 (C-N, C-Ostretching) cm^{-1}.

*Dimethyl 7-oxo-7H-benzo[de]benzo[4,5]imidazo[2,1-a]isoquinoline-11,12-dicarboxylate (***4b***)* Yield: 76 %; Melting point: 158–160 °C; Mass m/z: 387.38 $[M+H]^+$;^1H NMR (DMSO-d_6, 600 MHz): δ 8.98 (d, 1H, Ar-H, *J*=7.2 Hz), 8.84 (d, 1H, Ar-H, *J*=7.2 Hz),8.66 (d, 1H, Ar-H, *J*=8.4 Hz),8.35 (d, 1H, Ar-H, *J*=8.4 Hz),8.21 (d, 1H, Ar-H, *J*=7.8 Hz),8.15 (d, 1H, Ar-H, *J*=9.0 Hz), 7.85 (m, 2H, Ar-H),4.14 (s, 3H, -OCH_3), 3.97 (s, 3H, -OCH_3);FTIR: 1718, 1704 (C=O stretching), 1609, 1591 (C=C, C=N stretching), 1532, 1465 (C-Caromatic stretching), 1331, 1318, 1265 (C-N, C-Ostretching) cm^{-1}.

Results and Discussion

Optimized Geometries

The geometries of the compounds were optimized at B3LYP/6-31+G(d) level. The optimized geometries can be understood with the help of the basic structure as shown in Fig. 1.This conclude that the two nitrogen atoms forming the imidazole or pyrimidine unit (designated as C-core in Fig. 1) is anchored on one side with the carbonyl aryl core of anhydrides (designated as A-core in Fig. 1) and other side aryl core of the 1,2-diamine (designated as D-core in Fig. 1). The dihedral angles of the C-core in ground state and excited state are influenced by the nature of the substituents on both the cores as well as the nature of the anhydride (phthalic or naphthalic).This is directly affecting the extent of planarity of the molecule and hence the charge transfer characteristics of the system.

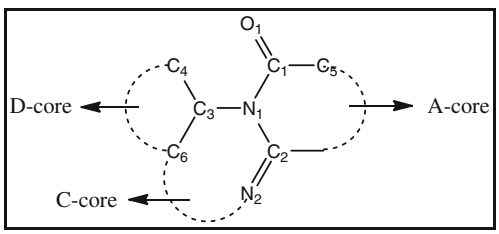

Fig. 1 General structure for all the compounds

As a representative example, the structural view of the compound **3b** in the ground and the excited state is presented in Table 1, Fig. 2. In the compound 3b the major bond lengthening was observed between the bonds C_1-C_5, C_1-C_{42}, C_2-C_3, C_4-C_5, N_{15}-C_{22}, N_{21}-C_{23}, C_{22}-O_{24}, C_{25}-C_{26}, C_{32}-C_{37}, C_{36}-C_{33} by 0.026, 0.023, 0.015, 0.096, 0.015, 0.053, 0.018, 0.033, 0.037, 0.036 Å and the bond length shortening for the bonds C_1-N_{21}, C_2-C_{42}, N_{15}-C_{23}, C_{22}-C_{26}, C_{23}-C_{32}, C_{25}-C_{30}, C_{28}-C_{33}, C_{36}-C_{37} by 0.045, 0.016, 0.016, 0.030, 0.044, 0.016, 0.006, 0.026 Å. Such a lengthening and shortening of the bonds were observed due to the effect of donor and acceptor groups present in the molecules. In the excited state, twist dihedral angle of the diester moiety of the donor core was reduced to maintain planarity. Similar changes in the geometries were observed in the optimized geometries at the ground and excited state of the remaining compounds **3a, 4a** and **4b** (Table 1).

The Mulliken charge distribution in the ground and the excited state (DCM solvent) of the compounds are summarized in Table 2. In the excited state of the compound **3b,** the net positive charge on the atom C_5 and C_6 increases from 0.525 to 0.557 and 0.073 to 0.119. While the net negative charge on N_{15} and C_{25} atom increases from −0.219 to −0.241 and −0.387 to −0.471 respectively (in au) (Fig. 3), which is suggestive of the charge delocalization in the molecule from the D-core to the A-core.

Photo-Physical Properties

To evaluate the effect of the solvent polarities on the photophysical properties of the polycyclic fused benzimidazole derivatives (**3a–3b** and **4a–4b),** absorption and emission were studied in five different solvents of differing polarity, dielectric constant, refractive indices and the results are summarized in Table 3, Figs. 4 and 5. The absorption as well as emission properties of the fused benzimidazole compounds were found to be nearly same in all the solvents studied. From this it was clear that, both the properties are independent of the solvent polarity. All of the compounds show a well-resolved absorption profile in the range of 305–385 nm with molar extinction coefficient values (ε) in agreement with π-π* transitions (Figs. 4 and 5). The computed vertical excitation values of the compounds are in good agreement with the experimental absorption and emission; the difference between

Table 1 Computed interatomic distance of the compounds **3a, 3b, 4a** and **4b** in ground and excited state in DMF

Bond.	**3a**		Bond.	**3b**		Bond.	**4a**		Bond.	**4b**	
	GS[a]	ES[b]		GS[a]	ES[b]		GS[a]	ES[b]		GS[a]	ES[b]
C_1-C_5	1.421	1.466	C_1-C_5	1.413	1.440	C_1-C_2	1.398	1.416	C_1-C_2	1.401	1.427
C_2-C_{36}	1.400	1.384	C_2-C_{42}	1.398	1.383	C_1-C_6	1.421	1.467	C_1-C_6	1.414	1.440
C_2-C_6	1.497	1.503	C_3-C_4	1.398	1.402	C_1-N_{24}	1.404	1.356	C_1-N_{24}	1.388	1.342
C_3-C_4	1.402	1.385	C_5-N_{15}	1.396	1.388	C_3-C_4	1.412	1.440	C_3-C_4	1.413	1.427
C_5-N_{15}	1.388	1.346	C_6-O_{16}	1.221	1.220	C_6-N_{18}	1.388	1.344	C_5-C_6	1.394	1.387
C_6-O_{16}	1.220	1.218	C_6-O_{19}	1.343	1.339	C_8-O_{22}	1.347	1.336	C_6-N_{18}	1.396	1.387
C_6-O_{19}	1.342	1.337	N_{15}-C_{22}	1.408	1.423	C_{13}-O_{20}	1.212	1.217	C_{13}-O_{20}	1.217	1.216
N_{15}-C_{28}	1.415	1.436	N_{15}-C_{23}	1.406	1.390	C_{13}-O_{21}	1.343	1.334	C_{13}-O_{21}	1.337	1.333
N_{15}-C_{29}	1.397	1.429	C_{17}-O_{41}	1.220	1.220	N_{18}-C_{32}	1.399	1.429	N_{18}-C_{25}	1.409	1.427
O_{17}-C_{35}	1.220	1.220	C_{18}-O_{41}	1.341	1.337	N_{18}-C_{31}	1.415	1.437	N_{18}-C_{26}	1.407	1.389
N_{21}-C_{29}	1.304	1.346	N_{21}-C_{23}	1.313	1.366	N_{24}-C_{32}	1.300	1.346	N_{24}-C_{26}	1.312	1.365
C_{22}-C_{23}	1.413	1.461	C_{22}-O_{24}	1.226	1.243	C_{25}-C_{26}	1.412	1.461	C_{25}-O_{27}	1.225	1.244
C_{23}-C_{24}	1.389	1.416	C_{22}-C_{26}	1.477	1.447	C_{25}-C_{31}	1.499	1.447	C_{25}-C_{29}	1.477	1.446
C_{23}-C_{29}	1.463	1.401	C_{23}-C_{32}	1.450	1.405	C_{25}-C_{30}	1.387	1.400	C_{26}-C_{35}	1.450	1.406
C_{25}-C_{24}	1.404	1.381	C_{26}-C_{27}	1.427	1.423	C_{26}-C_{32}	1.463	1.401	C_{29}-C_{30}	1.427	1.424
C_{25}-C_{26}	1.400	1.428	C_{27}-C_{32}	1.425	1.438	C_{28}-C_{29}	1.401	1.428	C_{30}-C_{35}	1.425	1.437
C_{26}-C_{27}	1.404	1.393	C_{32}-C_{37}	1.390	1.427	C_{29}-C_{30}	1.403	1.393	C_{35}-C_{40}	1.389	1.426

Bond distances are in Å

[a] Bond distances were obtained at the optimized ground state geometry

[b] Bond distances were obtained at the optimized excited state geometry

the computed and experimental values is less than 30 nm in all the solvents studied and 52 nm (in DMF) respectively.

The red shifted absorption maxima of the compounds **3b** and **4b** indicates that the naphthalic anhydride (385 nm in DMF) has a stronger electron withdrawing effect than in **3a** and **4a** (321, and 328 nm in DMF). Similarly the compounds **3b** and **4b** showed red shifted emission as compared to the compounds **3a** and **4a**. Introduction of the substituent on the donor core (D-core) induced intramolecular charge transfer and mesomeric dipole moment. When compared with unsubstituted analogues [49] of the compounds **3a** and **4a** latter have shown a blue shifted absorption but in compounds **3b** and **4b** nearly the same. The electron withdrawing effect of diester groups on donor core have not induced efficient donor to acceptor charge transfer. The compounds **3a** and **4a** absorbs at shorter wavelength in DCM as compared to their unsubstituted analogue which absorb at 340 nm, while compounds **3b** and **4b** absorb at the same wavelength (384 nm) due to strong withdrawing effect of naphthalene core. Also in the case of emission the unsubstituted analogue in DCM are

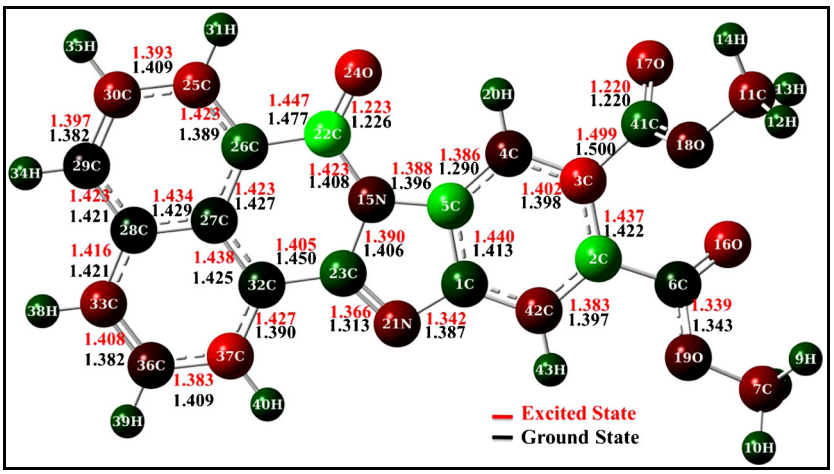

Fig. 2 Optimized geometry parameters of the compound **3b** in DMF solvent in the ground state and excited state (bond lengths are in Å, angles are in degree)

Table 2 Mulliken charge (e) distribution for compounds **3a, 3b, 4a** and **4b** in the ground state (GS) and excited state (ES) optimized geometry in DCM

Atom	**3a**		**3b**		Atom	**4a**		**4b**	
	GS	ES	GS	ES		GS	ES	GS	ES
C_1	−0.126	−0.236	0.332	0.224	C_1	0.173	0.238	0.213	0.255
C_3	−0.136	−0.031	−0.559	−0.560	C_3	−0.068	−0.057	−0.197	−0.177
C_5	0.562	0.614	0.525	0.557	C_5	−0.779	−0.684	−0.888	−0.847
C_6	0.512	0.373	0.073	0.119	C_6	0.763	0.700	0.706	0.706
N_{15}	−0.204	−0.199	−0.219	−0.241	N_{18}	−0.206	−0.198	−0.261	−0.261
O_{16}	−0.496	−0.483	−0.500	−0.501	O_{19}	−0.551	−0.545	−0.563	−0.566
O_{19}	−0.259	−0.227	−0.271	−0.273	O_{22}	−0.329	−0.323	−0.332	−0.329
N_{21}	−0.414	−0.392	−0.361	−0.360	N_{24}	−0.366	−0.346	−0.296	−0.297
C_{23}	−0.265	−0.374	0.143	0.276	C_{25}	0.099	0.155	0.814	0.871
C_{25}	−0.191	−0.213	−0.387	−0.471	C_{26}	0.071	−0.044	0.363	0.214
C_{26}	−0.279	−0.268	0.224	0.267	C_{28}	−0.147	−0.149	−0.466	−0.273
C_{27}	−0.434	−0.400	0.091	0.109	C_{29}	−0.289	−0.281	0.401	0.115
$O_{34/24}$	−0.549	−0.548	−0.568	−0.561	C_{30}	−0.527	−0.524	0.117	0.029
$C_{35/41}$	0.281	0.375	0.295	0.270	C_{32}	0.709	0.637	−0.064	0.058
$C_{36/42}$	−0.359	−0.365	−0.367	−0.349	O_{37}/C_{35}	−0.538	−0.542	0.206	0.143

red shifted (519 and 499 nm) as compared to the compounds **3a–4a** and **3b–4b** respectively.

Relative Quantum Yield

The fluorescence quantum yields of the synthesized polycyclic fused benzimidazole derivatives were determined in different solvents and tabulated in Table 3. The nature of the substituent and the solvent polarity are mostly affecting the fluorescence quantum yields of the compounds. Here, it has been observed that the compounds **3a–3b** and **4a–4b** enhances the fluorescence quantum yields in the polar aprotic (DMF) and non polar (THF) solvents respectively. The highest quantum yield of the compounds **3a–3b** in DMF and **4a–4b** in THF was observed. The values in the increasing order are: **3a** (0.13) < **3b** (0.26) and < **4a** (0.11) < **4b** (0.25). The quantum yield values were the lowest in methanol in the increasing order: **4a** (0.05) < **3a** (0.07) < **4b** (0.10) < **3b** (0.15).

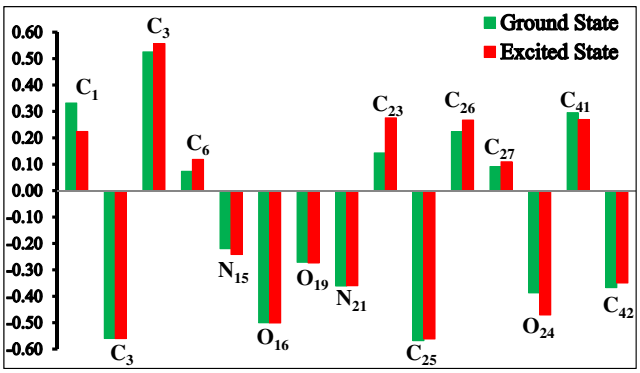

Fig. 3 The ground state (GS) and excited state (ES) Mulliken charge (e) distribution of the compound **3b** in DCM

Electronic Vertical Excitations (TD-DFT)

The electronic vertical excitations were calculated using TD-B3LYP/6-31+G(d) method. Table 3 is summarized the experimental absorption wavelengths and the computed vertical excitation spectra associated with their oscillator strengths, orbital composition, and their corresponding assignments for the compounds **3a–3b** and **4a–4b.** The absorption band of the compounds occurring at the lower energy with higher oscillator strength is due to the intramolecular charge transfer (ICT) and it is the characteristic of the donor-acceptor chromophore. These ICT bands mainly occur due to the electronic transition from the highest occupied molecular orbital HOMO and HOMO-1 to the lowest unoccupied molecular orbital (LUMO) of the compounds **3a–4a** and **3b–4b** respectively. Both the experimental absorption and the computed vertical excitation of the compounds **3a–3b** and **4a–4b** are independent of the solvent polarity. The percent deviation between the experimental and the computed absorption of the compounds **3a, 3b, 4a** and **4b** in DCM is 6.1, 6.5, 5.6 and 7.2 % respectively. As an example of the compound **3b**, in the case of non polar solvent like THF, HOMO to LUMO (98 %) transition is responsible for the vertical excitation located at 411 nm with oscillator strength (*f*) 0.44, which corresponds to the experimentally observed absorption peak at 387 nm (Table 3).

Frontier Molecular Orbital

The effects of the charge transfer from dimethyl phthalate (D-core) to the carbonyl chromophore (A-core) were studied to understand the electronic transition and the charge delocalization within the molecules. The first dipole allowed electron

Table 3 Observed UV-Visible absorption-emission and its computed vertical excitation spectra of absorption-emission of the compounds **3a, 3b, 4a** and **4b** in different solvents

Comp.	Solvents	Experimental			Computed (TD-DFT)						Φ
		λ_{max}[a] nm ( )	λ_{max}[b] nm intensity(au)	Stokes shift	Vertical[c] Exct. (nm)	f[d]	Orbital contribution	%D[e]	TD-DFT emission (nm)	%D[f]	
3a	THF	312(21,701)	409(27.45)	97	330	0.12	H-1→L(88 %)	5.8	———	———	0.08
	DCM	310(19,728)	407(24.21)	97	329	0.13	H-1→L(88 %)	6.1	———	———	0.07
	MeOH	305(22,669)	425(63.65)	120	330	0.11	H-1→L(88 %)	8.2	———	———	0.07
	ACN	326(23,276)	408(49.33)	82	330	0.11	H-1→L(88 %)	1.1	———	———	0.10
	DMF	321(26,069)	410(60.67)	89	331	0.12	H-1→L(88 %)	3.1	399	2.7	0.13
3b	THF	387(20,878)	472(310.94)	85	411	0.44	H→L (98 %)	6.2	———	———	0.23
	DCM	386(18,790)	473(252.98)	87	411	0.44	H→L (98 %)	6.5	———	———	0.18
	MeOH	381(21,965)	478(180.97)	97	409	0.43	H→L (97 %)	7.4	———	———	0.15
	ACN	385(22,156)	469(212.67)	84	409	0.43	H→L (97 %)	6.3	———	———	0.17
	DMF	385(29,782)	471(236.28)	86	411	0.45	H→L (97 %)	6.6	423	3.0	0.26
4a	THF	291(50,410) 321(33,208)	402(35.69)	111 81	339	0.12	H-1→L(84 %)	5.7	———	———	0.11
	DCM	291(41,661) 321(27,321)	402(32.09)	111 81	339	0.13	H-1→L(84 %)	5.6	———	———	0.08
	MeOH	289(39,564) 321(25,787)	399(15.73)	110 78	337	0.11	H-1→L(84 %)	5.1	———	———	0.05
	ACN	295(43,916) 325(28,791)	412(35.48)	117 87	337	0.11	H-1→L(84 %)	3.8	———	———	0.08
	DMF	295(39,564) 328(24,958)	412(43.78)	117 84	338	0.12	H-1→L(84 %)	3.9	394	4.4	0.08
4b	THF	381(16,812)	477(327.55)	96	410	0.47	H→L (98 %)	7.5	———	———	0.25
	DCM	382(18,475)	477(247.96)	95	410	0.47	H→L (98 %)	7.2	———	———	0.12
	MeOH	379(17,825)	483(164.64)	104	407	0.46	H→L (97 %)	7.4	———	———	0.1
	ACN	381(22,290)	471(197.43)	90	407	0.46	H→L (97 %)	6.9	———	———	0.14
	DMF	385(20,081)	473(243.63)	88	405	0.50	H→L (97 %)	5.3	421	3.9	0.16

[a] Experimental absorption wavelength

[b] Experimental emission wavelength

[c] Computed absorption wavelength

[d] Oscillator strength

[e] % Deviation between experimental absorption and vertical excitation computed by DFT

[f] % Deviation between experimental emission and computed (TD-DFT) emission

Φ: Quantum yield at various solvents

——— Not calculated

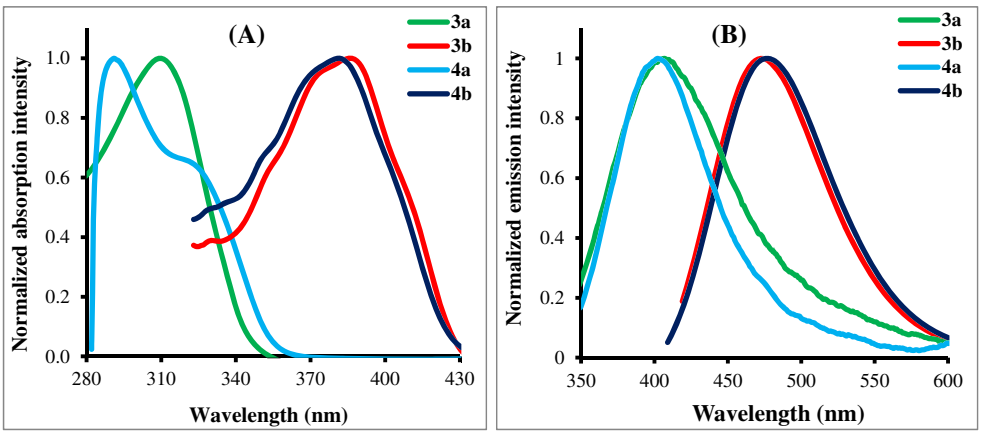

Fig. 4 Normalized **(a)** absorption and **(b)** emission intensity of the compounds **3a, 3b, 4a** and **4b** in DCM

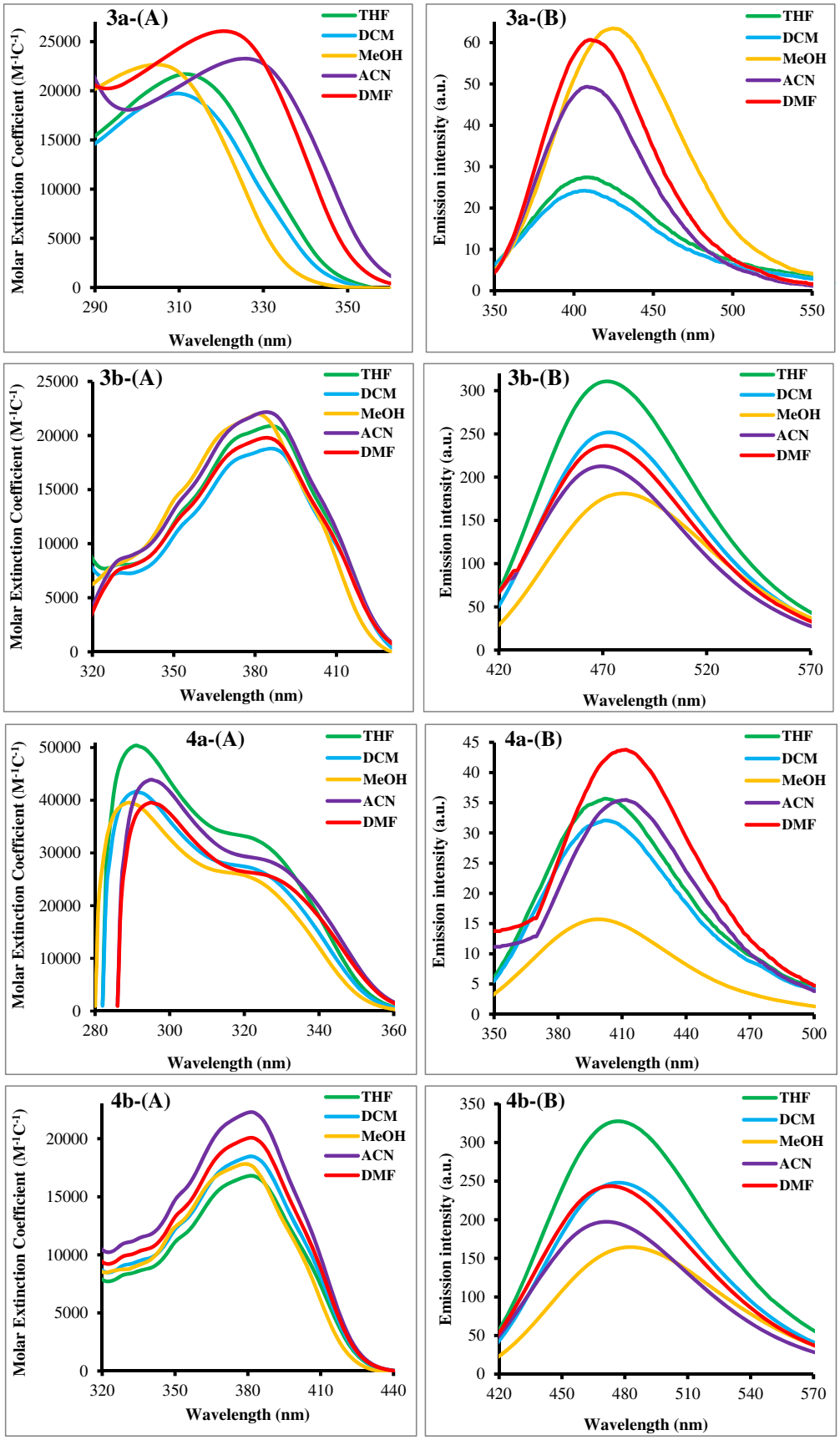

Fig. 5 **a** Absorption and **b** emission of the compounds **3a, 3b, 4a** and **4b** in different solvent

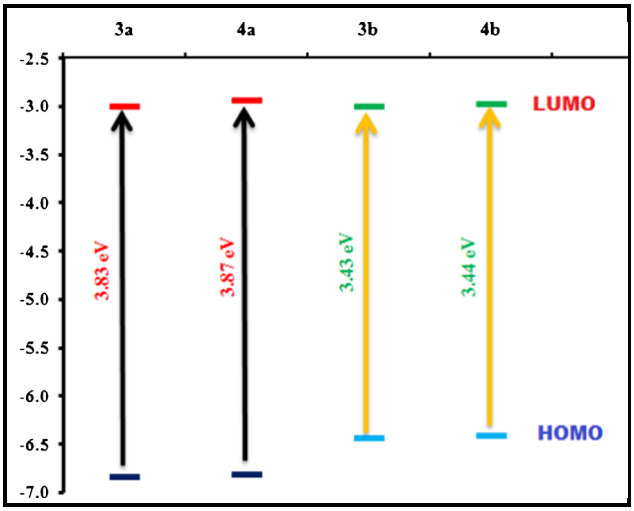

Fig. 6 Energy gap between HOMO→LUMO of the compounds **3a, 3b, 4a** and **4b** in DMF solvents

transition and the strongest electron transitions usually correspond almost exclusively to the ICT of an electron from HOMO→LUMO or HOMO-1→LUMO energies of different molecular orbitals in different solvents are illustrated in Tables S1-S2. In the case of the entire solvents energy gap between the HOMO -1→LUMO and HOMO -1→LUMO orbital of the compounds **3a–4a** and **3b–4b** nearly same as the solvent polarity was increased or decreased respectively (Table S1-S2). The HOMO and LUMO energy level of the compounds **3a** and **4a** in DMF remains same, and it may be due to the very similar reduction potential. Similarly in the case of compounds **3b** and **4b (Fig. 6)**. This is understandable because of these structural isomer having same reduction site [50].

Figure 7 displays the energies of the different molecular orbitals involved in the electronic transitions of the compounds **3a–3b** and **4a–4b** in dichloromethane obtained from the B3LYP-optimized geometries. It clearly shows that in the HOMO, the whole electron density lies on the two nitrogen atoms and the donor (Core-D) ring, which gets shifted on the carbonyl group and the C-core (Figs. 1 and 2) in the LUMO. This indicates the charge transfer behavior of the compounds where the electrons get pulled from the donor to the acceptor end. In LUMO there is no electron density on the nitrogen in each case and it possesses a node.

Static Second-Order Nonlinear Optical (NLO) Properties

The D-A chromophores probably having good non-linear properties and their first hyperpolarizability (β_o) values can be enhanced due to their relative orientation. Thus, their good linear and nonlinear optical properties of the asymmetrical D-A chromophores have been studied. Density functional theory (DFT) was used to calculate the second-order NLO properties of the polycyclic benzimidazole D-A chromophores. The static first hyperpolarizability (β_o) and its related properties for the compounds were calculated using B3LYP/6-31+G(d) on the basis of the finite field approach [51]. The computed first hyperpolarizability (β_o) values were found to be ranging from 95.15, 107.76, 70.08, 67.16×10^{-31} e.s.u. for the compounds **3a, 3b, 4a** and **4b** respectively. The computed β-tensors are summarized in Table 4. These values are significantly greater than the values for urea (3.8×10^{-31} e.s.u.) by 24, 28, 18 and 17 times respectively. These compounds have shown a large hyperpolarizability, significantly considerable charge transfer characteristics of the ground state to the first excited state. This is further supported by the large variation in

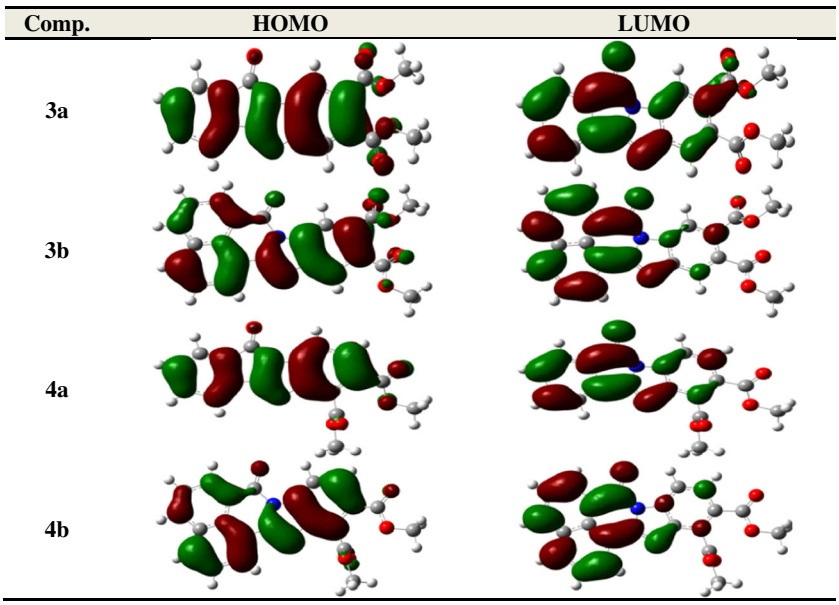

Fig. 7 Frontier molecular orbitals of the compounds **3a, 3b, 4a** and **4b** in DCM solvent

Table 4 Static first hyperpolarizability and its β -components of the compounds **3a, 3b, 4a** and **4b** (all values in e.s.u.)

β-tensors	**3a**	**3b**	**4a**	**4b**
β_{xxx}	-3.21×10^{-30}	9.65×10^{-30}	3.21×10^{-30}	1.35×10^{-30}
β_{xxy}	-1.70×10^{-30}	-1.09×10^{-30}	5.40×10^{-30}	3.74×10^{-30}
β_{xyy}	-5.66×10^{-31}	$1.27E\times10^{-30}$	1.62×10^{-30}	2.98×10^{-30}
β_{yyy}	-1.91×10^{-32}	-5.42×10^{-31}	-3.36×10^{-31}	1.21×10^{-30}
β_{xxz}	3.06×10^{-30}	1.93×10^{-32}	3.10×10^{-31}	-9.53×10^{-32}
β_{yyz}	9.74×10^{-32}	2.20×10^{-31}	-2.07×10^{-31}	4.00×10^{-32}
β_{xzz}	-2.77×10^{-30}	-2.62×10^{-31}	-1.84×10^{-31}	1.33×10^{-32}
β_{yzz}	-1.42×10^{-30}	1.64×10^{-31}	1.72×10^{-31}	1.78×10^{-31}
β_{zzz}	2.99×10^{-30}	-5.17×10^{-32}	-2.03×10^{-31}	1.08×10^{-31}
β_o	95.15×10^{-31}	107.76×10^{-31}	70.08×10^{-31}	67.16×10^{-31}

the dipole moments between the ground and the excited states from the solvatochromism studies. From these observations it was clear that, these compounds could be used as promising candidates in the field of non-linear optics.

Conclusion

In summary, we have designed and synthesized the novel D-A type chromophores containing the dimethyl phthalate (D-core) as an electron donor and carbonyl chromophore (A-core) as the electron acceptors. The structures of the synthesized fused polycyclic benzimidazole were confirmed by FT-IR, ^{1}H-NMR, ^{13}C-NMR and Mass spectral analysis. The resultant photophysical data revealed that these compounds have a high Stokes shift ranging from 78 to 120 nm. The significant emissive property implies that the electronic coupling between the donor and the acceptor was sufficient to allow a charge transfer within the molecule and they are sensitive towards the solvent polarity. The quantum yield of the compounds **4a–4b** was observed to be comparatively higher in non-polar solvent while compounds **3a–3b** in polar solvent.

The geometry of the fused polycyclic benzimidazole derivatives were optimized at B3LYP/6-31+G(d) level. The vertical excitations and emissions were computed and are in good agreement with the experimental results. The compounds **3a–4a** and **3b–4b** have shown a prominent absorption due to HOMO-1→LUMO and HOMO→LUMO transition with a high oscillator strength respectively. The isodensity orbital plots have displayed that majority of the electron density in HOMO is located on the dimethyl phthalate (D-core). The first hyperpolarizability was calculated by using the finite field approach at B3LYP/6-31+G(d) level and it was found that these compounds possess a large second-order nonlinear property as compared to urea. These compounds could be used as promising candidates for various applications in nonlinear optics (NLO), electronic-photonic devices and organic light emitting diodes.

Acknowledgments The authors are greatly thankful to TIFR, SAIF-I.I.T. Mumbai for recording the ^{1}H-NMR and Mass spectra. One of the authors Mininath S. Deshmukh is grateful to CSIR for financial support.

References

1. Meltesics W, Sternbach H (1975) 2-{8 2-(1,3-Diazacycloalk-2-enyl{9 benzophenone derivatives and 1,3-diazacycloalkenyl{8 2,1-a{9 isoindole derivatives, US3905994A
2. Meltesics W, Sternbach H (1975) Novel 2{8 2-(1,3-diazacycloalk-2-enyl){9 benzophenone derivatives and novel 1,3-diazacycloalkenyl{8 2,1-A{9 isoindole derivatives, US3929766A
3. Geigy JR (1967) NL6613264A
4. Graf W (1970) Verfahren zur Herstellung von neuen, kondensierten heterocyclischen Verbindungen, CH482697A
5. Aeberli P, Eden P, Gogerty JH et al (1975) Anorectic agents. 2. Structural analogs of 5-(p-chlorophenyl)-2,3-dihydro-5H-imidazo[2,1-a]isoindol-5-ol. J Med Chem 18:182–185
6. Aeberli P, Eden P, Gogerty JH et al (1975) 5-Aryl-2,3-dihydro-5H-imidazo[2,1-a]isoindol-5-ols. Novel class of anorectic agents. J Med Chem 18:177–182
7. Sulkowski TS (1972) Benzodiazocines, US3663532A
8. Sulkowski TS (1976) 5H-Imidazo{8 2,1-a{9 isoindol-5-one compounds, US3994920A
9. Sulkowski TS (1973) Imidazolinyl phenyl carbonyl acid addition salts and related compounds, US3763178A
10. Ashkar SA-K (1978) Method for inhibiting bud growth of plants, US4093441A
11. Los M (1978) Dihydroimidazoisoindoldione und verfahren zu ihrer herstellung, DE2700269A1
12. Ashkar SA-K (1978) Method for controlling the relative stem growth of plants, US4067718A
13. Ashkar SA-K (1978) Method for inhibiting bud growth of plants, US4090860A
14. Waud W, Harrison S Jr, Gilbert K et al (1991) Antitumor drug cross-resistance in vivo in a cisplatin-resistant murine P388 leukemia. Cancer Chemother Pharmacol 27:456–463
15. Dzierzbicka K, Trzonkowski P, Sewerynek P, Myśliwski A (2003) Synthesis and cytotoxic activity of conjugates of Muramyl and Normuramyl dipeptides with batracylin derivatives. J Med Chem 46:978–986
16. Meegalla SK, Stevens GJ, McQueen CA et al (1994) Synthesis and pharmacological evaluation of Isoindolo[1,2-b]quinazolinone and Isoindolo[2,1-a]benzimidazole derivatives related to the antitumor agent batracylin. J Med Chem 37:3434–3439
17. Herbst W, Hunger K, Wilker G et al (2004) Industrial organic pigments: production, properties, applications, third edit. WILEY-VCH Verlag GmbH & Co. KGaA, Weinheim
18. Mizuguchi J (2004) Crystal structure and electronic characterization of trans and cis Perinone pigments. J Phys Chem B 108:8926–8930
19. Zhan X, Facchetti A, Barlow S et al (2011) Rylene and related diimides for organic electronics. Adv Mater 23:268–284
20. Mishra A, Fischer MKR, Bäuerle P (2009) Metal-free organic dyes for dye-sensitized solar cells: from structure: property relationships to design rules. Angew Chem Int Ed 48:2474–2499
21. Zhao Y, Di C, Gao X et al (2011) All-solution-processed, high-performance n-channel organic transistors and circuits: toward low-cost ambient electronics. Adv Mater 23:2448–2453

22. Singh VP, Singh RS, Parthasarathy B et al (2005) Copper-phthalocyanine-based organic solar cells with high open-circuit voltage. Appl Phys Lett 86:82103–82106
23. Li Y, Zhang G, Yang G et al (2013) Extended π-conjugated molecules derived from naphthalene diimides toward organic emissive and semiconducting materials. J Org Chem 78:2926–2934
24. Dhagat P, Haverinen HM, Kline RJ et al (2009) Influence of dielectric surface chemistry on the microstructure and carrier mobility of an n-type organic semiconductor. Adv Funct Mater 19:2365–2372
25. Hu Y, Gao X, Di C et al (2011) Core-expanded naphthalene diimides fused with sulfur heterocycles and end-capped with electron-withdrawing groups for air-stable solution-processed n-channel organic thin film transistors. Chem Mater 23:1204–1215
26. Xue J, Uchida S, Rand BP, Forrest SR (2004) Asymmetric tandem organic photovoltaic cells with hybrid planar-mixed molecular heterojunctions. Appl Phys Lett 85:5757–5759
27. Ahmed E, Ren G, Kim FS et al (2011) Design of new electron acceptor materials for organic photovoltaics: synthesis, electron transport, photophysics, and photovoltaic properties of oligothiophene-functionalized naphthalene diimides. Chem Mater 23:4563–4577
28. Tang CW (1986) Two-layer organic photovoltaic cell. Appl Phys Lett 48:183–185
29. Babel A, Jenekhe SA (2003) High electron mobility in ladder polymer field-effect transistors. J Am Chem Soc 125:13656–13657
30. Baeg K-J, Khim D, Jung S-W et al (2012) Remarkable enhancement of hole transport in top-gated N-Type polymer field-effect transistors by a high-k dielectric for ambipolar electronic circuits. Adv Mater 24: 5433–5439
31. Chang J, Ye Q, Huang K et al. (2012) Stepwise cyanation of naphthalene diimide for n-channel field-effect transistors. 2010–2013
32. Sophy KB, Calaminici P, Pal S (2007) Density functional static dipole polarizability and first-hyperpolarizability calculations of Nan (n=2, 4, 6, 8) clusters using an approximate CPKS method and its comparison with MP2 calculations†. J Chem Theory Comput 3:716–727
33. Brouwer AM (2011) Standards for photoluminescence quantum yield measurements in solution (IUPAC Technical Report). Pure Appl Chem 83:2213–2228
34. Treutler O, Ahlrichs R (1995) Efficient molecular numerical integration schemes. J Chem Phys 102:346
35. Becke A (1993) A new mixing of Hartree-Fock and local density functional theories. J Chem Phys 98:1372
36. Lee C, Yang W, Parr RG (1988) Development of the Colle-Salvetti correlation-energy formula into a functional of the electron density. Phys Rev B 37:785–789
37. Kim CH, Park J, Seo J et al (2010) Excited state intramolecular proton transfer and charge transfer dynamics of a 2-(2′-Hydroxyphenyl)benzoxazole derivative in solution. J Phys Chem A 114:5618–5629
38. Santra M, Moon H, Park M-H et al (2012) Dramatic substituent effects on the photoluminescence of boron complexes of 2-(Benzothiazol-2-yl)phenols. Chem Eur J 18:9886–9893
39. Casida ME, Jamorski C, Casida KC, Salahub DR (1998) Molecular excitation energies to high-lying bound states from time-dependent density-functional response theory: characterization and correction of the time-dependent local density approximation ionization threshold. J Chem Phys 108:4439
40. Li H, Niu L, Xu X et al (2011) A comprehensive therotical investigation of intramolecular proton transfer in the excited states for some newly-designed diphenylethylene derivatives bearing 2-(2-Hydroxy-Phenyl)-benzotriazole part. J Fluoresc 21:1721–1728
41. Bauernschmitt R, Ahlrichs R (1996) Treatment of electronic excitations within the adiabatic approximation of time dependent density functional theory. Chem Phys Lett 256:454–464
42. Furche F, Rappoport D (2005) Density functional theory for excited states: equilibrium structure and electronic spectra. In Computational Photochemistry. In: Olivucci M (ed) Comput. Photochem. Amsterdam: Elsevier, p 93
43. Wiberg KB (1986) Ab Initio molecular orbital theory by W. J. Hehre, L. Radom, P. v. R. Schleyer, and J. A. Pople, John Wiley, New York, 548 pp. Price: 79.95 (1986). J Comput Chem 7:379
44. Lakowicz JR (1999) Principles of fluorescence spectroscopy, 2nd edn. Kluwer, New York
45. Valeur B (2001) Molecular fluorescence: principles and applications. Wiley-VCH Verlag GmbH, Weinheim
46. Cossi M, Barone V, Cammi R, Tomasi J (1996) Ab initio study of solvated molecules: a new implementation of the polarizable continuum model. Chem Phys Lett 255:327–335
47. Frisch MJ, Trucks GW, Schlegel HB et al. (2009) Gaussian 09 C.01
48. Williams RL, Shalaby SW (1973) Heterocyclic studies: new heterocyclic ring systems from isomeric dimethyl diaminophthalates. J Heterocycl Chem 10:891–898
49. Mamada M, Pérez-Bolívar C, Anzenbacher P (2011) Green synthesis of polycyclic benzimidazole derivatives and organic semiconductors. Org Lett 13:4882–4885
50. Chen C-T, Chiang C-L, Lin Y-C et al (2003) Ortho-substituent effect on fluorescence and electroluminescence of arylamino-substituted coumarin and stilbene. Org Lett 5:1261–1264
51. Vidya S, Ravikumar C, Hubert Joe I et al (2011) Vibrational spectra and structural studies of nonlinear optical crystal ammonium D, L-tartrate: a density functional theoretical approach. J Raman Spectrosc 42:676–684